Assistant Vehicle Localization Based on Three Collaborative Base Stations via SBL-Based Robust DOA Estimation

Assistant Vehicle Localization Based on Three Collaborative Base Stations via SBL-based Robust DOA Estimation

Huafei Wang, Liangtian Wan, *Member, IEEE,* Mianxiong Dong, *Member, IEEE,* Kaoru Ota, *Member, IEEE,* and Xianpeng Wang, *Member, IEEE*

***Abstract*—As a promising research area in Internet of Things (IoT), Internet of Vehicles (IoV) has attracted much attention in wireless communication and network. In general, vehicle localization can be achieved by the Global Positioning Systems (GPS). However, in some special scenarios, such as cloud cover, tunnels or some places where the GPS signals are weak, GPS cannot perform well. The continuous and accurate localization services cannot be guaranteed. In order to improve the accuracy of vehicle localization, an assistant vehicle localization method based on Direction-of-Arrival (DOA) estimation is proposed in this paper. The assistant vehicle localization system is composed of three Base Stations (BS) equipped with a Multiple Input Multiple Output (MIMO) array. The locations of vehicles can be estimated if the positions of the three BSs and the DOAs of vehicles estimated by the BSs are known. However, the DOA estimated accuracy maybe degrade dramatically when the electromagnetic environment is complex. In the proposed method, a Sparse Bayesian Learning (SBL) based robust DOA estimation approach is first proposed to achieve the off-grid DOA estimation of the target vehicles under the condition of non-uniform noise, where the covariance matrix of non-uniform noise is estimated by a Least Squares (LS) procedure, and a grid refinement procedure implemented by finding the roots of a polynomial is performed to refine the grid points to reduce the off-grid error. Then, according to the DOA estimation results, the target vehicle is cross-located once by each two BSs in the localization system. Finally, robust localization can be realized based on the results of three-time cross-location. Plenty of simulation results demonstrate the effectiveness and superiority of the proposed method.**

***Index Terms*—Vehicle localization, Base station, Off-grid error, Non-uniform noise, Direction-of-arrival estimation, Sparse Bayesian learning**

I. Introduction

With the rapid development of economy and automatic driving technology, the number of mobile devices such as autonomous vehicles [1], [2] has increased dramatically in Internet of Things (IoT). The vehicle localization is becoming more and more important for Internet of Vehicles (IoV) [3], [4] since the data transmission is based on accurate location information of vehicles. Generally, vehicle localization can be accurately achieved by the cooperation between Global Positioning Systems (GPS) and motion sensors on the vehicles in most scenarios when the GPS is available [5]. However, GPS is not always available anywhere. Therefore, it is particularly important to exploit an assistant localization system, which may be composed of radars or sensors [6], [7], to achieve vehicle localization. The Received Signal Strength Indication (RSSI) technique has been adopted widely [8], [9], [10] to achieve target vehicle localization. However, most of the RSSI-based algorithms need to know the spatial fading characteristics of signals [11], [12], [13], which is difficult to obtain accurately due to the complexity of wireless channel. In addition, some Time Difference of Arrival (TDOA) based algorithms [14], [15] are arisen, but their performance is highly sensitive to time difference measurement, which makes it hard to achieve high accuracy vehicle localization. Aiming at this, the Direction-of-Arrival (DOA) based target localization methods [16], [17] become a good choice. Compare with the RSSI and TDOA, the DOA-based localization methods are just dependent on the accuracy of DOA estimation, which is easily obtained by the plenty exist DOA estimation algorithms.

For DOA estimation, a lot of excellent methods have been proposed based on the subspace technique, such as Multiple Signal Classification (MUSIC) [18], [19] algorithm and Estimation of Signal Parameters via Rotational Invariance Techniques (ESPRIT) [20]. Further, some Reduced-Complexity (RC) methods, such as root-MUSIC [21], RC-MUSIC [22] and RC-ESPRIT [23], are reported for reducing the computational complexity of the subspace based algorithms. However, only when the Signal-to-Noise Ratio (SNR) and snapshot number are large enough, these subspace-based algorithms can achieve the required DOA estimation performance. When the SNR is low and/or the snapshot number is limited, their performance may decrease significantly. To overcome these limitations, the Sparse Signal Representation (SSR) technique has emerged as a new DOA estimation technique. Based on the advantages of SSR technique, amounts of SSR-based methods have been presented for DOA estimation, including l_1-norm optimization based algorithm [24], [25] and Sparse Bayesian Learning (SBL) based algorithm [26], [27]. Compared with the l_1-norm optimization based algorithm, the SBL-based methods are paid

H. Wang and X. Wang are with State Key Laboratory of Marine Resource Utilization in South China Sea, College of Information Science and Technology, Hainan University, Haikou, 570228, China (e-mail: wong9525@163.com; wxpeng1986@126.com)

L. Wan is with Key Laboratory for Ubiquitous Network and Service Software of Liaoning Province, School of Software, Dalian University of Technology, Dalian, 116620, China (e-mail: wanliangtian@dlut.edu.cn).

M. Dong and K. Ota are with Department of Information and Electronic Engineering, Muroran Institute of Technology, Muroran, 050-8585, Japan (e-mail: {mx.dong; ota}@csse.muroran-it.ac.jp).

Corresponding author: Xianpeng Wang; e-mail: wxpeng1986@126.com

more attention by scholars because of their small estimation error and better estimation performance [28].

However, it is known that the SBL-based methods usually obtain the sparsity of the signal by discretizing the spatial range, which will form a uniform discrete grid, and then DOA estimation can be realized by using the maximum likelihood criterion or the maximum posterior probability criterion. However, without a suitable discrete grid, which is difficult to select in practice, it is hard for SBL-based method to achieve the satisfied DOA estimation performance [29]. A dense enough grid will lead to heavy computation complexity. It is unavailable for all true DOAs to exactly locate on the discrete grid points, and then the off-grid error must exist between the true DOA and its nearest grid point. Aiming at solving the off-grid DOA estimation problem, a Sparse Total Least Squares (STLS) solution is proposed in [30], where the off-grid gap is supposed to follow a Gaussian prior distribution, and the error is approximated by the first order Taylor expansion of the true DOA at the grid point closest to it. In addition, a new method called Off-Grid Sparse Bayesian Inference (OGSBI) [31], in which the off-grid error is supposed to obey a uniform distribution within the grid interval, is proposed to achieve the off-grid DOA estimation by linear approximation. Furthermore, a block-sparse Bayesian learning method [32], where the noise variance does not need to be estimated, is presented to realize the off-grid DOA estimation by utilizing the covariance matrix of received data. However, both of these two methods in [31] and [32] achieve the satisfied off-grid DOA estimation performance at the expense of computational complexity, and their performances are still unsatisfied under a very coarse grid condition. Therefore, in order to achieve satisfied performance with relatively low computational complexity and a coarse grid, the root sparse Bayesian learning algorithm for off-grid DOA estimation (ROGSBL) is reported in [33], in which the spatial grid is refined by solving a polynomial. Nevertheless, the process of solving polynomial in [33] is still computationally inefficient. Hence, to further improve the efficiency of the grid updating procedure, an enhanced SBL method [34] is proposed to realize the off-grid DOA estimation, where the grid point is dynamically updated by a forgotten factor model.

On the other hand, all the algorithms mentioned above for off-grid DOA estimation are based on the assumption that the noise is uniform Gaussian white noise which is unrealistic to meet in practice due to the non-uniform sensor response and non-ideal receiving channel [35], [36]. Aiming at dealing with the non-uniform noise, a large number of Maximum Likelihood (ML) based algorithms [37]-[40] have been proposed in the past few decades. Particularly, the stochastic ML method presented in [40] can effectively eliminate the influence of non-uniform noise by accurately estimating the covariance matrix of non-uniform noise based on a modified inverse iteration algorithm. However, the requirement of ML algorithm for joint search makes it unfavorable for practical application. On the other hand, the SSR-based algorithms [41]-[44] for DOA estimation under non-uniform noise condition also attract great attention. By utilizing the modified inverse iteration algorithm in [40] to estimate the covariance of non-uniform noise, an improved SBL-based algorithm is presented in [41] to realize DOA estimation with non-uniform noise. Besides, considering the second-order statistical information of the received signal, several covariance matrix based methods [42], [43] are investigated to achieve DOA estimation in non-uniform noise, and the high precision DOA estimation can be achieved in [43] based on an adaptive procedure [29]. However, the performance of the method proposed in [43] may suffer from aperture loss and can be further improved. Moreover, by adopting the Least Squares (LS) strategy, a SBL-based method [44], which is suitable for non-uniform noise is proposed to achieve DOA estimation. It is not difficult to find that all the algorithms mentioned above either consider the presence of non-uniform noise or the off-grid error. However, in order to improve the DOA estimation accuracy in complexly practical environment, the coexisting of non-uniform noise and off-grid error have to be tackled efficiently.

In this paper, an assistant vehicle localization method based on a SBL-based robust DOA estimation approach in the co-existence of non-uniform noise and off-grid error is proposed, where the assistant vehicle localization system is composed of three collaborative Base Stations (BSs) equipped with Multiple Input Multiple Output (MIMO) array. In the proposed DOA estimation method, the received data of BS is firstly compressed by a transformation matrix. Then a sparse model is established for off-grid DOA estimation, where the variance of echo signal is estimated by Expectation Maximization (EM) algorithm. The noise power, which is always non-uniform noise after dimensional reduction, is estimated by a LS strategy, and the discrete grid point is refined by the EM algorithm which is performed by solving a polynomial. Finally, the off-grid DOA estimation can be realized by performing a one Dimension (1D) spectrum search of the echo signal on the refined discrete grid. Extensive simulation results indicate that the proposed method can maintain superior localization performance based on the excellent performance of the proposed robust DOA estimation approach under the coexistence of non-uniform noise and off-grid error, especially under the condition of a very coarse grid.

The main contributions of this paper are summarized as follows:

1) A vehicle localization system consisting of three collaborative BSs equipped with MIMO array is presented. Each two of the three BSs can cross-locate the target vehicle once, and three results of cross-location can be obtained. The final localization result is obtained by the average of three cross-location results, which enables the proposed method to achieve more stable localization performance.
2) The collaborative BS is composed of MIMO array which can expand array aperture effectively, and the spatial diversity makes radar signal processing achieve more Degree of Freedom (DOF). These advantages make MIMO array obtain higher spatial angle resolution for DOA estimation, improve the accuracy of angle estimation effectively, and increase the maximum number of discernible targets significantly.
3) A SBL-based robust DOA estimation approach is pro-

posed under the coexistence of non-uniform noise and off-grid error. The LS strategy is adopted to estimate the variance of non-uniform noise, and a grid refinement is performed by finding roots of a polynomial to update the discrete grid. Thus the DOA estimation approach can effectively handle the influence of non-uniform noise and off-grid error simultaneously. As a result, the proposed DOA estimation approach can maintain more accurate and stable localization performance under the coexistence of non-uniform noise and off-grid error. On the other hand, compare with the subspace-based method, the proposed SBL-based approach is less sensitive to SNR and snapshot number, and can maintain superior performance of DOA estimation under small SNR or/and low snapshot number.

4) The grid refinement procedure in the proposed DOA estimation approach can effectively reduce the off-grid error, especially in the very coarse grid case. Without affecting the performance of DOA estimation, the coarser the grid partitions, the faster the DOA estimation speed achieves. In addition, by selecting an appropriate number of "active" grid points, the DOA estimation speed can be improved further. Plenty of simulations are conducted to verify the superiority and effectiveness of the proposed approach.

The definition of some important notations used in this paper are given in the following Table I.

TABLE I
SOME IMPORTANT NOTATIONS

Notations	Definition
capital bold letters	the matrices
lowercase bold letters	the vectors
$(\cdot)^T$	the transpose operation
$(\cdot)^H$	the conjugate transpose operation
$(\cdot)^{-1}$	the inverse operation
$\mathrm{E}\{\cdot\}$	find the mathematical expectation
$diag\{\cdot\}$	the diagonalization operation
$\mathbb{C}^{M\times N}$	the $M \times N$ complex matrix set
$\otimes$	the Kronecker product
$\mathrm{tr}(\cdot)$	return the trace of a matrix
$\min(\cdot)$	return the minimum value of a set
$\|\cdot\|_F$	the Frobenius norm
$\|\cdot\|_2$	the 2-norm
$\|\cdot\|$	the absolute value

II. LOCALIZATION SYSTEM AND DATA MODEL

As shown in Fig. 1, consider an assistant vehicle localization system with three collaborative BSs consisting of a large number of antennas, where the BS is equipped with MIMO array. This is reasonable since a large number of antennas can be used for constructing the MIMO array. All the three BSs

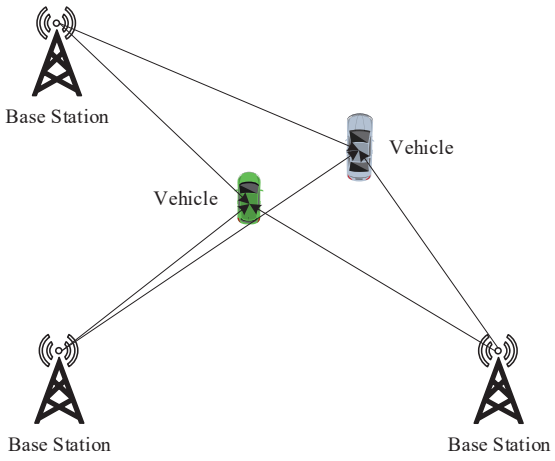

Fig. 1. Vehicle localization system with three collaborative base stations

are configured and work in the same way. The BS estimates the DOA of the target vehicle, and each two BSs cross-locate the target vehicle based on the DOA estimation results. The accurate localization can be ultimately achieved through the three results from cross-localization. Each BS consists of transmitting array and receiving array, and the transmitting array and receiving array are colocated, which means that the DOA of a vehicle is identical for the transmitting array and receiving array. Both transmitting array and receiving array are uniform linear array (ULA), and the distance between adjacent antennas is half-wavelength. Suppose that the transmitting array and receiving array are composed of M and N antennas, respectively. There exist K target vehicles in the same plane range, θ_k represents the DOA of the kth target where $k = 1, 2, \cdots, K$. The transmitting array of BS emits M orthogonal waveforms and the receiving array collects the echo signal reflected by the target vehicles. Then the echo signal received by receiving array of the BS at the tth snapshot can be expressed as [18]

$$\tilde{\boldsymbol{x}}(t) = \sum_{k=1}^{K} s_k(t)\boldsymbol{a}_r(\theta_k)\boldsymbol{a}_t^T(\theta_k)\boldsymbol{\Omega} + \tilde{\boldsymbol{n}}(t), \tag{1}$$

where $s_k(t) = \xi_k(t)e^{j2\pi f_k(t)}$ represents the echo signal reflected by the kth target vehicle, $\xi_k(t)$ and $f_k(t)$ stand for the reflection coefficient and the Doppler frequency, respectively. $\boldsymbol{\Omega} = [\omega_1, \omega_2, \cdots, \omega_M]^T$ is the complex code matrix of M orthogonal waveforms emitted by transmitting array, where $\omega_m (m = 1, 2, \cdots .M)$ represents the complex code vector transmitted by the mth transmitting antenna. When $i = j$, the waveforms satisfy $\omega_i^H \omega_j = 1$, and when $i \neq j$, they satisfy $\omega_i^H \omega_j = 0$. $\tilde{\boldsymbol{n}}(t)$ represents the unknown non-uniform Gaussian white noise vector and its covariance can be expressed as $\tilde{\boldsymbol{Q}} = \mathrm{E}\{\tilde{\boldsymbol{n}}(t)\tilde{\boldsymbol{n}}(t)^H\} = diag\{\sigma_1^2, \sigma_2^2, \ldots, \sigma_N^2\}$, where σ_n^2 is the variance of noise received by the nth receiving antenna and $\sigma_1^2 \neq \sigma_2^2 \neq \ldots \neq \sigma_N^2$. $\boldsymbol{a}_t(\theta_k)$ and $\boldsymbol{a}_r(\theta_k)$ respectively represent the transmit steering vector and receive steering vector with $\boldsymbol{a}_t(\theta_k) = [1, e^{-j\pi \sin\theta_k}, \ldots, e^{-j\pi(M-1)\sin\theta_k}]^T$ and $\boldsymbol{a}_r(\theta_k) = [1, e^{-j\pi \sin\theta_k}, \ldots, e^{-j\pi(N-1)\sin\theta_k}]^T$. After matching filtering, the output data at the receiving array of the BS can

be expressed as

$$\boldsymbol{x}(t) = \boldsymbol{A}\boldsymbol{s}(t) + \boldsymbol{n}(t), \tag{2}$$

where $\boldsymbol{x}(t) \in \mathbb{C}^{MN\times 1}$ is the output data vector at the tth snapshot. $\boldsymbol{A} = [\boldsymbol{a}_t(\theta_1)\otimes\boldsymbol{a}_r(\theta_1),\cdots,\boldsymbol{a}_t(\theta_K)\otimes\boldsymbol{a}_r(\theta_K)]$ represents the transmit-receive joint steering matrix. And $\boldsymbol{s}(t) = [s_1(t), s_2(t),\cdots,s_K(t)]^T$ is the echo signal vector. $\boldsymbol{n}(t)$ denotes the noise vector after matched filtering, which is still non-uniform noise. The covariance matrix of $\boldsymbol{n}(t)$ is shown as

$$\boldsymbol{Q} = \mathrm{E}\{\boldsymbol{n}(t)\boldsymbol{n}(t)^H\} = \boldsymbol{I}_M \otimes \tilde{\boldsymbol{Q}}. \tag{3}$$

Collecting T snapshots, the output data in Eq. (2) can be formulated as the matrix form as follows

$$\boldsymbol{X} = \boldsymbol{A}\boldsymbol{S} + \boldsymbol{N}, \tag{4}$$

where $\boldsymbol{X} = [\boldsymbol{x}(1),\boldsymbol{x}(2),\ldots,\boldsymbol{x}(T)]$, $\boldsymbol{S} = [\boldsymbol{s}(1),\boldsymbol{s}(2),\ldots,\boldsymbol{s}(T)]$, and $\boldsymbol{N} = [\boldsymbol{n}(1),\boldsymbol{n}(2),\ldots,\boldsymbol{n}(T)]$.

By observing the structure of the joint steering matrix $\boldsymbol{A}$, it can be found that the joint steering vector $\boldsymbol{a}_t(\theta_k)\otimes\boldsymbol{a}_r(\theta_k) \in \mathbb{C}^{MN\times 1}$. However, there are only $P = M + N - 1$ unique entries in it, which means that there exist some redundant entries in it. Considering the existence of redundant entries in the joint steering vector, it can be rewritten as

$$\boldsymbol{a}_t(\theta_k)\otimes\boldsymbol{a}_r(\theta_k) = \boldsymbol{J}\times\boldsymbol{b}(\theta_k), \tag{5}$$

where $\boldsymbol{b}(\theta_k) = [1, e^{-j\pi\sin\theta_k},\ldots,e^{-j\pi(P-1)\sin\theta_k}]^T$ is the new steering vector, and $\boldsymbol{J}\in\mathbb{C}^{MN\times P}$ is expressed as

$$\boldsymbol{J} = \begin{bmatrix}
1 & 0 & \cdots & 0 & 0 & \cdots & 0 \\
0 & 1 & \cdots & 0 & 0 & \cdots & 0 \\
\vdots & \vdots & \ddots & \vdots & \vdots & \ddots & \vdots \\
0 & 0 & \cdots & 1 & 0 & \cdots & 0 \\
0 & 1 & 0 & \cdots & 0 & \cdots & 0 \\
0 & 0 & 1 & \cdots & 0 & \cdots & 0 \\
\vdots & \vdots & \vdots & \ddots & \vdots & \ddots & \vdots \\
0 & 0 & 0 & \cdots & 1 & \cdots & 0 \\
\vdots & \vdots & \vdots & \vdots & \vdots & \vdots & \vdots \\
0 & \cdots & 0 & 1 & 0 & \cdots & 0 \\
0 & \cdots & 0 & 0 & 1 & \cdots & 0 \\
\vdots & \ddots & \vdots & \vdots & \vdots & \ddots & \vdots \\
0 & \cdots & 0 & 0 & 0 & \cdots & 1
\end{bmatrix} \tag{6}$$

Hence, the data model in Eq.(4) can be rewritten as

$$\boldsymbol{X} = \boldsymbol{J}\boldsymbol{B}\boldsymbol{S} + \boldsymbol{N}, \tag{7}$$

where $\boldsymbol{B} = [\boldsymbol{b}(\theta_1),\boldsymbol{b}(\theta_2),\cdots,\boldsymbol{b}(\theta_K)]$ is the new steering matrix without redundant entries. It should be noticed that it is inappropriate to directly multiply $\boldsymbol{J}^H$ with Eq. (7) to reduce the dimension, which will transform the noise into color noise [34]. On the other hand, we can find that

$$\boldsymbol{J}^H\boldsymbol{J} = \mathrm{diag}(1,2,\cdots,\underbrace{\min(M,N),\cdots,\min(M,N)}_{|M-N|+1},\cdots,2,1), \tag{8}$$

which is a full rank matrix. Hence, in order to remove the redundant entries and achieve the purpose of dimensionality reduction, the following transformation matrix is constructed

$$\boldsymbol{D} = (\boldsymbol{J}^H\boldsymbol{J})^{-1}\boldsymbol{J}^H. \tag{9}$$

By multiplying the transformation matrix $\boldsymbol{D}$ with the data model in Eq. (7), we have

$$\boldsymbol{Y} = \boldsymbol{D}\boldsymbol{J}\boldsymbol{B}\boldsymbol{S} + \boldsymbol{D}\boldsymbol{N} = \boldsymbol{B}\boldsymbol{S} + \boldsymbol{E}, \tag{10}$$

where $\boldsymbol{Y} = [\boldsymbol{y}(1),\boldsymbol{y}(2),\ldots,\boldsymbol{y}(T)]$. $\boldsymbol{E} = \boldsymbol{D}\boldsymbol{N}$ is still the unknown non-uniform noise, and its covariance matrix is shown as

$$\bar{\boldsymbol{Q}} = \mathrm{E}\{(\boldsymbol{D}\boldsymbol{n}(t))(\boldsymbol{D}\boldsymbol{n}(t))^H\} = diag\{\bar{\sigma}_1^2,\bar{\sigma}_2^2,\ldots,\bar{\sigma}_P^2\} \tag{11}$$

where $\bar{\sigma}_p^2(p = 1,2,\cdots,P)$ can be regarded as the converted noise power. Obviously, whether the received noise at the receiving array is uniform or non-uniform, the converted noise must be non-uniform noise.

Generally, according to the sparse representation strategy, the plane range from -90° to 90° where target vehicle is located is uniformly fixed into $\bar{K}$ parts with $\bar{K} \gg P > K$. Then a discrete grid will be formed in the plane and a complete direction set $\bar{\boldsymbol{\vartheta}} = [\vartheta_1,\vartheta_2,\cdots,\vartheta_{\bar{K}}]$ can be obtained. Obviously, if the complete direction set is dense enough, the vehicles are sparse on it. Then the sparse signal model of Eq. (10) can be expressed as

$$\boldsymbol{Y} = \bar{\boldsymbol{B}}\bar{\boldsymbol{S}} + \boldsymbol{E} \tag{12}$$

where $\bar{\boldsymbol{B}} = [\boldsymbol{b}(\vartheta_1),\boldsymbol{b}(\vartheta_2),\cdots,\boldsymbol{b}(\vartheta_{\bar{K}})] \in \mathbb{C}^{P\times\bar{K}}$ is the overcomplete dictionary with $\boldsymbol{b}(\vartheta_{\bar{k}}) = [1, e^{-j\pi\sin\vartheta_{\bar{k}}},\ldots,e^{-j\pi(P-1)\sin\vartheta_{\bar{k}}}]^T(\bar{k} = 1,2,\cdots,\bar{K})$. And $\bar{\boldsymbol{S}} = [\bar{\boldsymbol{s}}(1),\bar{\boldsymbol{s}}(2),\ldots,\bar{\boldsymbol{s}}(T)]$, where $\bar{\boldsymbol{s}}(t) = [s_1(t),s_2(t),\cdots,s_{\bar{K}}(t)]^T$ is a K sparse signal vector. According to the sparse signal model in Eq. (12), the DOA estimation of vehicles can be achieved by estimating the parameters of the sparse signal vector.

III. SBL-BASED ROBUST DOA ESTIMATION

A. Sparse Bayesian framework

Based on the statistical Sparse Bayesian Learning (SBL) strategy [26], each column of the sparse matrix $\bar{\boldsymbol{S}}$ is supposed to follow the independent complex Gaussian distribution in this paper, i.e.,

$$\bar{\boldsymbol{s}}(t) \sim \mathcal{CN}(\boldsymbol{0},\boldsymbol{\Upsilon}), \tag{13}$$

where $\mathcal{CN}(\boldsymbol{0},\boldsymbol{\Upsilon})$ represents the complex Gaussian distribution with zero mean and variance $\boldsymbol{\Upsilon} = diag(\boldsymbol{\gamma})$. $\boldsymbol{\gamma} = [\gamma_1,\gamma_2,\cdots,\gamma_{\bar{K}}]^T$ is known as the hyper-parameter set, and $\gamma_{\bar{k}}$ denotes the variance of echo signal from the direction $\vartheta_{\bar{k}}$. Since $\bar{\boldsymbol{S}}$ contains the echo signal of T snapshots, its probability density distribution can be calculated as

$$p(\bar{\boldsymbol{S}}|\boldsymbol{\gamma}) = \prod_{t=1}^{T}\mathcal{CN}(\bar{\boldsymbol{s}}(t)|\boldsymbol{0},\boldsymbol{\Upsilon}). \tag{14}$$

In addition, the entries of $\boldsymbol{\gamma}$ are assumed to follow the independent Gamma distribution, i.e., $\gamma_{\bar{k}} \sim \Gamma(\alpha,\beta)$, with

$\bar{k} = 1, 2, \cdots, \bar{K}$. Then the probability density distribution of $\boldsymbol{\Upsilon}$ can be obtained as

$$p(\boldsymbol{\Upsilon}) = \prod_{\bar{k}=1}^{\bar{K}} \Gamma(\gamma_{\bar{k}}|\alpha, \beta), \tag{15}$$

where $\Gamma(\gamma_{\bar{k}}|\alpha,\beta) = \Gamma(\gamma_{\bar{k}})^{-1}\beta^{\alpha}\gamma_{\bar{k}}^{\alpha-1}e^{-\beta\gamma_{\bar{k}}}$ with $\Gamma(\gamma_{\bar{k}}) = \int_0^{\infty} t^{\gamma_{\bar{k}}-1}e^{-t}dt$. Generally, α and β are two constants close to zero [26].

According to the above assumptions and Bayesian principle, it is easy to deduce that the received data $\boldsymbol{Y}$ also follows the complex Gaussian distribution. Hence, the probability density function of $\boldsymbol{Y}$ is

$$\begin{aligned} p(\boldsymbol{Y}|\bar{\boldsymbol{S}}, \bar{\boldsymbol{Q}}) &= \prod_{t=1}^{T} \mathcal{CN}(\boldsymbol{y}(t)|\bar{\boldsymbol{B}}\bar{\boldsymbol{s}}(t), \bar{\boldsymbol{Q}}) \\ &= |\pi\bar{\boldsymbol{Q}}|^{-T}\exp\{-\mathrm{tr}[(\boldsymbol{Y}-\bar{\boldsymbol{B}}\bar{\boldsymbol{S}})^H\bar{\boldsymbol{Q}}^{-1}(\boldsymbol{Y}-\bar{\boldsymbol{B}}\bar{\boldsymbol{S}})]\}. \end{aligned} \tag{16}$$

Then by utilizing the Bayesian derivation, the posterior probability density of $\bar{\boldsymbol{S}}$ can be calculated as

$$\begin{aligned} p(\bar{\boldsymbol{S}}|\boldsymbol{Y}; \boldsymbol{\gamma}, \bar{\boldsymbol{Q}}) &= \frac{p(\boldsymbol{Y}|\bar{\boldsymbol{S}}; \bar{\boldsymbol{Q}})p(\bar{\boldsymbol{S}}|\boldsymbol{\gamma})}{\int p(\boldsymbol{Y}|\bar{\boldsymbol{S}}; \bar{\boldsymbol{Q}})p(\bar{\boldsymbol{S}}|\boldsymbol{\gamma})d\bar{\boldsymbol{S}}} \\ &= |\pi\boldsymbol{\Sigma}|^{-T}\exp\{-\mathrm{tr}[(\bar{\boldsymbol{S}}-\boldsymbol{\mu})^H\boldsymbol{\Sigma}^{-1}(\bar{\boldsymbol{S}}-\boldsymbol{\mu})]\}, \end{aligned} \tag{17}$$

where $\boldsymbol{\mu}$ and $\boldsymbol{\Sigma}$ respectively represent the mean and covariance, which are calculated as

$$\boldsymbol{\mu} = \boldsymbol{\Upsilon}\bar{\boldsymbol{B}}^H(\bar{\boldsymbol{Q}} + \bar{\boldsymbol{B}}\boldsymbol{\Upsilon}\bar{\boldsymbol{B}}^H)^{-1}\boldsymbol{Y}, \tag{18}$$

$$\boldsymbol{\Sigma} = \boldsymbol{\Upsilon} - \boldsymbol{\Upsilon}\bar{\boldsymbol{B}}^H(\bar{\boldsymbol{Q}} + \bar{\boldsymbol{B}}\boldsymbol{\Upsilon}\bar{\boldsymbol{B}}^H)^{-1}\bar{\boldsymbol{B}}\boldsymbol{\Upsilon}. \tag{19}$$

In order to estimate $\boldsymbol{\mu}$ and $\boldsymbol{\Sigma}$, the hyper-parameter $\boldsymbol{\gamma}$ and the non-uniform noise covariance matrix $\bar{\boldsymbol{Q}}$ should be estimated first. The posterior probability density distribution of $\boldsymbol{Y}$ with respect to $\boldsymbol{\gamma}$ and $\bar{\boldsymbol{Q}}$ can be calculated as follows

$$\begin{aligned} p(\boldsymbol{Y}|\boldsymbol{\gamma}, \bar{\boldsymbol{Q}}) &= \int p(\boldsymbol{Y}|\bar{\boldsymbol{S}}, \bar{\boldsymbol{Q}})p(\bar{\boldsymbol{S}}|\boldsymbol{\gamma})d\bar{\boldsymbol{S}} \\ &= |\pi\boldsymbol{\Sigma}_{\boldsymbol{Y}}|^{-T}\exp\{-\mathrm{tr}(\boldsymbol{Y}^H\boldsymbol{\Sigma}_{\boldsymbol{Y}}^{-1}\boldsymbol{Y})\}, \end{aligned} \tag{20}$$

where $\boldsymbol{\Sigma}_{\boldsymbol{Y}} = \bar{\boldsymbol{Q}} + \bar{\boldsymbol{B}}\boldsymbol{\Upsilon}\bar{\boldsymbol{B}}^H$. Obviously, it is a type-II maximum likelihood problem for the estimation of $\boldsymbol{\gamma}$ and $\bar{\boldsymbol{Q}}$. By taking the logarithm of Eq. (20) and neglecting the constant terms, the objective likelihood function for estimating hyper-parameter $\boldsymbol{\gamma}$ is shown as follows

$$\mathcal{L}(\boldsymbol{\gamma}, \bar{\boldsymbol{Q}}) = \ln|\boldsymbol{\Sigma}_{\boldsymbol{Y}}| + \mathrm{tr}(\boldsymbol{\Sigma}_{\boldsymbol{Y}}^{-1}\hat{\boldsymbol{R}}), \tag{21}$$

where $\hat{\boldsymbol{R}} = \frac{1}{T}\boldsymbol{Y}\boldsymbol{Y}^H$ is a substitute for $\boldsymbol{R} = \mathrm{E}[\boldsymbol{y}(t)\boldsymbol{y}^H(t)]$, because the ideal $\boldsymbol{R}$ is unrealistic to obtain in practice.

B. Estimation of echo signal and non-uniform noise power

To estimate the hyper-parameter $\boldsymbol{\gamma}$, we just have to minimize the objective likelihood function in Eq. (21). Generally, the Expectation Maximization (EM) algorithm is adopted to optimize the objective likelihood function and achieve the estimation of $\boldsymbol{\gamma}$. Hence, according to the strategy of EM algorithm, the partial derivative of Eq. (21) with respect to $\boldsymbol{\gamma}$ is taken and we set it to be zero, i.e.,

$$\frac{\partial\mathcal{L}(\boldsymbol{\gamma}, \bar{\boldsymbol{Q}})}{\partial\boldsymbol{\gamma}} = 0. \tag{22}$$

Then, by solving Eq. (22), the updating formula for $\boldsymbol{\gamma}$ can be derived as $\gamma_{\bar{k}}^{(i)} = \frac{1}{T}\|(\boldsymbol{\mu}^{(i)})_{\bar{k}\cdot}\|_2^2 + (\boldsymbol{\Sigma}^{(i)})_{\bar{k},\bar{k}}$. However, in the process of convergence, most elements of $\boldsymbol{\gamma}$ tend to be zero due to its sparsity, which may lead to the calculation singularity. Therefore, in order to avoid this phenomenon, the updating formula for $\boldsymbol{\gamma}$ is revised as [28]

$$\gamma_{\bar{k}}^{(i)} = \frac{1}{T}\|(\boldsymbol{\mu}^{(i)})_{\bar{k}\cdot}\|_2^2 \Big/ \left[1 - \frac{(\boldsymbol{\Sigma}^{(i)})_{\bar{k},\bar{k}}}{\gamma_{\bar{k}}^{(i)}}\right] + \tau, \tag{23}$$

where $\bar{k} = 1, 2 \ldots, \bar{K}$. $(\cdot)_{\bar{k}}$ and $(\cdot)_{\bar{k},\bar{k}}$ represents the $\bar{k}$th entry of a vector and $(\bar{k},\bar{k})$th entry of a matrix, respectively. $\gamma_{\bar{k}}^{(i)}$, $\boldsymbol{\mu}^{(i)}$ and $\boldsymbol{\Sigma}^{(i)}$ denote the estimated results of $\gamma_{\bar{k}}$, $\boldsymbol{\mu}$ and $\boldsymbol{\Sigma}$ in the ith iteration, respectively, where $\boldsymbol{\mu}^{(i)}$ and $\boldsymbol{\Sigma}^{(i)}$ can be calculated by Eq. (18) and Eq. (19). τ is a small positive constant, such as $\tau = 10^{-10}$ [28].

On the other hand, $\bar{\boldsymbol{Q}}$ can also be estimated theoretically by optimizing the objective likelihood function in Eq. (21). However, it seems impossible to obtain the analytical estimation of $\bar{\boldsymbol{Q}}$ by optimizing the objective likelihood function in Eq. (21) through the partial derivative due to the non-uniformity of $\bar{\boldsymbol{Q}}$ [28]. Therefore, LS procedure is adopted to estimate the non-uniform noise covariance matrix $\bar{\boldsymbol{Q}}$. After each iteration, the crude estimation of K DOAs, which is denoted as $\hat{\boldsymbol{\vartheta}} = [\hat{\vartheta}_1, \hat{\vartheta}_2, \cdots, \hat{\vartheta}_K]$, can be obtained by the 1D spectrum search, and the corresponding steering matrix is $\hat{\boldsymbol{B}}_K = [\boldsymbol{b}(\hat{\vartheta}_1), \boldsymbol{b}(\hat{\vartheta}_2), \cdots, \boldsymbol{b}(\hat{\vartheta}_K)]$. Based on the theory in [44] and the knowledge of subspace technique, the subspace formed by the columns of $\boldsymbol{R}-\bar{\boldsymbol{Q}}$ and $\hat{\boldsymbol{B}}_K$ are the same subspace, which means

$$\boldsymbol{R} - \bar{\boldsymbol{Q}} = \hat{\boldsymbol{B}}_K\boldsymbol{H}, \tag{24}$$

where $\boldsymbol{R} = \mathrm{E}[\boldsymbol{y}(t)\boldsymbol{y}^H(t)]$, and $\boldsymbol{H}$ is a full rank matrix. The $p(p = 1, 2, \cdots, P)$th column of $\boldsymbol{R} - \bar{\boldsymbol{Q}}$ can be represented by $\boldsymbol{u}_p = \boldsymbol{v}_p - \bar{\sigma}_p^2\boldsymbol{e}_p$, where $\boldsymbol{v}_p$ denotes the pth column of $\boldsymbol{R}$ and $\boldsymbol{e}_p$ is a column vector with only the pth element is 1 and the other elements are 0. Then, the error between column vectors of $\boldsymbol{R} - \bar{\boldsymbol{Q}}$ and $\hat{\boldsymbol{B}}_K\boldsymbol{H}$ can be calculated by

$$g(p) = \|\boldsymbol{u}_p - \hat{\boldsymbol{B}}_K\boldsymbol{h}_p\|_2^2, \tag{25}$$

where $\boldsymbol{h}_p$ represents the pth column of $\boldsymbol{H}$. By utilizing the LS procedure to solve the Eq. (25), the LS solution of $\boldsymbol{h}_p$ can be obtained as $\boldsymbol{h}_p = (\hat{\boldsymbol{B}}_K^H\hat{\boldsymbol{B}}_K)^{-1}\hat{\boldsymbol{B}}_K^H\boldsymbol{u}_p$. Then, the objective function for estimating noise variance can be derived by substituting $\boldsymbol{h}_p$ back into $g(p)$ as follows

$$\ell(\bar{\sigma}_p^2) = \sum_{p=1}^{P}\|\boldsymbol{u}_p - \hat{\boldsymbol{B}}_K\boldsymbol{h}_p\|_2^2 = \sum_{p=1}^{P}\boldsymbol{u}_p^H\boldsymbol{\Pi}\boldsymbol{u}_p, \tag{26}$$

where $\boldsymbol{\Pi} = \boldsymbol{I}_P - \hat{\boldsymbol{B}}_K(\hat{\boldsymbol{B}}_K^H\hat{\boldsymbol{B}}_K)^{-1}\hat{\boldsymbol{B}}_K^H$. Then, the updating formula for the non-uniform noise covariance matrix $\bar{\boldsymbol{Q}}$ is derived by taking the partial derivation of $\ell(\bar{\sigma}_p^2)$ with respect

to $\bar{\sigma}_p^2$, i.e., $\partial \ell(\bar{\sigma}_p^2)/\partial \bar{\sigma}_p^2 = 0$. Thus, the updating formula for $\bar{\sigma}_p^2$ can be derived as

$$\bar{\sigma}_p^2 = \frac{\boldsymbol{e}_p^T \boldsymbol{\Pi} \boldsymbol{v}_p - \boldsymbol{v}_p^H \boldsymbol{\Pi} \boldsymbol{e}_p}{2\boldsymbol{e}_p^T \boldsymbol{\Pi} \boldsymbol{e}_p}. \tag{27}$$

Until now, the variance of echo signal and non-uniform noise can be estimated by Eq. (23) and Eq. (27), respectively. Based on the sparsity of $\bar{\boldsymbol{S}}$, the DOA estimation can be realized through the 1D spectrum search now. However, the obtained accuracy of DOA estimation is still seriously affected by the off-grid error. Especially, when the discrete grid is very coarse, the performance will be seriously degraded. Aiming at solving this problem, the off-grid DOA estimation with a coarse grid will be achieved by a grid refinement procedure in the following subsection.

C. Off-grid DOA estimation

Similar to the procedure in [33], the EM algorithm is used to refine the grid points. In E-step, the mathematical expectation of Eq. (16) is first calculated as follows

$$\begin{aligned} &\mathrm{E}_{p(\bar{\boldsymbol{S}}|\boldsymbol{Y};\boldsymbol{\gamma},\bar{\boldsymbol{Q}})}\{\ln(p(\boldsymbol{Y}|\bar{\boldsymbol{S}},\bar{\boldsymbol{Q}}))\} \\ &= -\sum_{t=1}^{T} \|\bar{\boldsymbol{Q}}^{-\frac{1}{2}}(\boldsymbol{y}_t - \bar{\boldsymbol{B}}\boldsymbol{\mu}_t)\|_2^2 - T\mathrm{tr}\left((\bar{\boldsymbol{Q}}^{-\frac{1}{2}}\bar{\boldsymbol{B}})\boldsymbol{\Sigma}(\bar{\boldsymbol{Q}}^{-\frac{1}{2}}\bar{\boldsymbol{B}})^H\right), \end{aligned} \tag{28}$$

where $\boldsymbol{y}_t$ and $\boldsymbol{\mu}_t$ represent the tth column of $\boldsymbol{Y}$ and $\boldsymbol{\mu}$, respectively. Then, in M-step, the mathematical expectation (i.e., Eq. (28)) of Eq. (16) is maximized. Let $\varphi_{\bar{k}} \triangleq e^{-j\pi \sin \vartheta_{\bar{k}}}$, and then we set the partial derivative of Eq. (28) with respect to $\varphi_{\bar{k}}$ to be 0, i.e.,

$$\begin{aligned} (\ddot{\boldsymbol{b}}_{\bar{k}}^{'})^H \Bigg(\ddot{\boldsymbol{b}}_{\bar{k}} \sum_{t=1}^{T} (|\boldsymbol{\mu}_{t,\bar{k}}|^2 + \varepsilon_{\bar{k},\bar{k}}) \\ + T\sum_{i\neq\bar{k}} \varepsilon_{i,\bar{k}} \ddot{\boldsymbol{b}}_i - \sum_{t=1}^{T} \boldsymbol{\mu}_{t,\bar{k}}^* \ddot{\boldsymbol{y}}_{t-\bar{k}} \Bigg) = 0, \end{aligned} \tag{29}$$

where $\ddot{\boldsymbol{b}}_{\bar{k}} = \bar{\boldsymbol{Q}}^{-\frac{1}{2}}\boldsymbol{b}_{\bar{k}}$ and $\ddot{\boldsymbol{b}}_{\bar{k}}^{'} = d\ddot{\boldsymbol{b}}_{\bar{k}}/d\varphi_{\bar{k}}$. $\boldsymbol{b}_{\bar{k}}$ denotes the $\bar{k}$th column of $\bar{\boldsymbol{B}}$. $\ddot{\boldsymbol{y}}_{t-\bar{k}} = \ddot{\boldsymbol{y}}_t - \sum_{i\neq\bar{k}} \boldsymbol{\mu}_{t,\bar{k}} \ddot{\boldsymbol{b}}_i$ with $\ddot{\boldsymbol{y}}_t = \bar{\boldsymbol{Q}}^{-\frac{1}{2}}\boldsymbol{y}_t$. $\boldsymbol{\mu}_{t,\bar{k}}$ denotes the $(t,\bar{k})$th element of $\boldsymbol{\mu}$, and $\varepsilon_{i,\bar{k}}$ is the $(i,\bar{k})$th element of $\boldsymbol{\Sigma}$. Then, by defining the following equation

$$\Phi^{(\bar{k})} \triangleq \sum_{t=1}^{T} (|\boldsymbol{\mu}_{t,\bar{k}}|^2 + \varepsilon_{\bar{k},\bar{k}}), \tag{30}$$

$$\Psi^{(\bar{k})} \triangleq T\sum_{i\neq\bar{k}} \varepsilon_{i,\bar{k}} \ddot{\boldsymbol{b}}_i - \sum_{t=1}^{T} \boldsymbol{\mu}_{t,\bar{k}}^* \ddot{\boldsymbol{y}}_{t-\bar{k}}, \tag{31}$$

Eq. (29) can be transformed into a polynomial form as

$$[\varphi_{\bar{k}}, 1, \varphi_{\bar{k}}^{-1}, \ldots, \varphi_{\bar{k}}^{-(P-2)}] \begin{bmatrix} \frac{P(P-1)}{2}\Phi^{(\bar{k})} \\ \Psi_2^{(\bar{k})} \\ 2\Psi_3^{(\bar{k})} \\ \vdots \\ (P-1)\Psi_P^{(\bar{k})} \end{bmatrix} = 0, \tag{32}$$

where $\Psi_p^{(\bar{k})}$ denotes the pth entry of $\Psi^{(\bar{k})}$. Since $|\varphi_{\bar{k}}| = 1$, the root with absolute value nearest to 1 in the $P-1$ roots is chosen to refine the grid point after solving the polynomial. The chosen root is represented by $\varphi_{\bar{k}^*}$, and then the $\bar{k}$th new grid point can be calculated by

$$\vartheta_{\bar{k}^*}^{ref} = \arcsin\left(-\frac{\lambda}{2\pi d} \cdot \mathrm{angle}(\varphi_{\bar{k}^*})\right). \tag{33}$$

Actually, when the true DOAs of vehicles overlap with the original grid points, the refinement procedure would inevitably reduce the accuracy of DOA estimation. Therefore, in order to avoid this negative impact, a further threshold is set to determine whether to refine the grid points or not as follows

$$\frac{\vartheta_{\bar{k}^*-1} + \vartheta_{\bar{k}^*}}{2} \leq \vartheta_{\bar{k}^*}^{ref} \leq \frac{\vartheta_{\bar{k}^*} + \vartheta_{\bar{k}^*+1}}{2}. \tag{34}$$

Now, a SBL-based robust DOA estimation approach under the coexistence of non-uniform noise and off-grid error has been proposed. The estimation of variance of echo signal and non-uniform noise can be obtained by an iterate procedure. The proposed method is summed up in Algorithm 1.

Algorithm 1 SBL-Based Robust DOA Estimation Approach

1: **Input:** The received data $\boldsymbol{X}$;
2: Construct the transformation matrix $\boldsymbol{D}$ according to Eq. (9);
3: Obtain $\boldsymbol{Y}$ according to Eq. (10);
4: **Initialization:** $\bar{\boldsymbol{Q}}$, $\boldsymbol{\gamma}$;
5: **while** $\sim$ Converge **do**
6: Update $\boldsymbol{\mu}$ and $\boldsymbol{\Sigma}$ by Eq. (18) and Eq. (19);
7: Update $\boldsymbol{\gamma}$ according to Eq. (23);
8: Update $\bar{\boldsymbol{Q}}$ according to Eq. (27);
9: Refine $\bar{\boldsymbol{\vartheta}}$ according to Eq. (32), Eq. (33) and Eq. (34)
10: **end while**
11: **Output:** $\bar{\boldsymbol{\vartheta}}$ and $\boldsymbol{\mu}$;
12: Achieve off-grid DOA estimation through 1D spectrum search on new $\bar{\boldsymbol{\vartheta}}$.

Remark 1: In step 4, $\bar{\boldsymbol{Q}}$ is initialized as $\bar{\boldsymbol{Q}} = (\bar{\sigma}^2)^{(0)}\boldsymbol{I}_P$ with $(\bar{\sigma}^2)^{(0)} = |\mathrm{tr}\{(\boldsymbol{I}_P - \bar{\boldsymbol{B}}\bar{\boldsymbol{B}}^H)\hat{\boldsymbol{R}}\}/(P-K)|$, where $\boldsymbol{I}_P$ denotes a $P \times P$ unit matrix. $\boldsymbol{\gamma}$ is initialized as $(\gamma_{\bar{k}})^{(0)} = \frac{1}{T}\|(\boldsymbol{\mu}^{(0)})_{\bar{k}\cdot}\|_2^2$ with $\boldsymbol{\mu}^{(0)} = \bar{\boldsymbol{B}}^H(\bar{\boldsymbol{B}}\bar{\boldsymbol{B}}^H)^{-1}\boldsymbol{Y}$.

Remark 2: The proposed robust DOA estimation method can maintain superior performance in the case of the coexistence of non-uniform noise and off-grid error, mainly caused by step 8 and step 9. In step 8, the variance of non-uniform noise can be accurately estimated. In step 9, the off-grid error can be minimized effectively. Actually, the refinement procedure in step 9 does not need to be implemented for every grid point in each iteration. In order to speed up the DOA estimation of the proposed algorithm, a proper number of "active" grid points are selected to be refined [33]. Define $f = \|\boldsymbol{\mu}_t\|_F$, and then the "active" grid points are determined according to the index of the first η maxima value of f, where $1 \leq \eta \leq P$. Usually, η is set to be $\eta \geq K$. When the number of signal is unknown, $\eta = P$ is recommended.

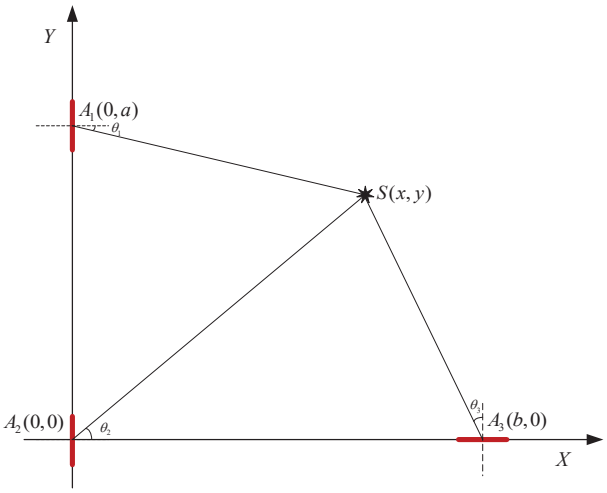

Fig. 2. Simplified diagram for vehicle localization with three collaborative base stations

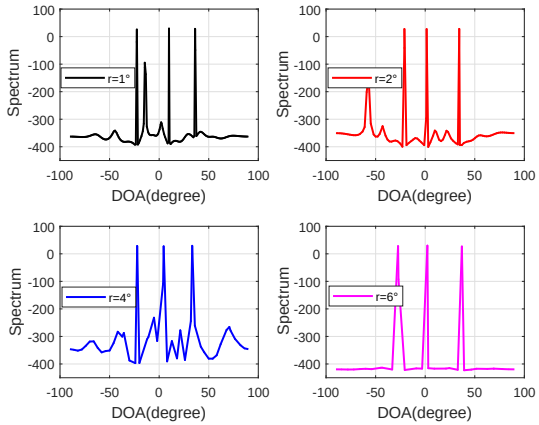

Fig. 3. Power spectrum under different grid intervals

IV. Vehicle Localization Based on DOA Estimation

For the sake of simplicity, the BSs in Fig. 1 are simplified to the bold red line as shown in Fig. 2, and the central antenna of BS is set as the reference point. The coordinates of reference points A_1, A_2 and A_3 corresponding to the three collaborative BSs are known to be $(0,a)$, $(0,0)$ and $(b,0)$, respectively. S is the position of the target vehicle, and its azimuth angles related to A_1, A_2 and A_3 are defined as θ_1, θ_2 and θ_3, respectively.

According to the measured data of BS A_1, A_2 and A_3, θ_1, θ_2 and θ_3 can be obtained by the robust DOA estimation approach in Algorithm 1, respectively. Then the following equation can be obtained as

$$\tan\theta_1 = \frac{a-y}{x}, \tag{35}$$

$$\tan\theta_2 = \frac{y}{x}, \tag{36}$$

$$\tan\theta_3 = \frac{b-x}{y}. \tag{37}$$

Based on Eq. (35) and Eq. (36), the target vehicle can be cross-located, and the coordinate of $S(x,y)$ can be calculated as

$$x_1 = \frac{a}{\tan\theta_1 + \tan\theta_2}, y_1 = \frac{a\tan\theta_2}{\tan\theta_1 + \tan\theta_2}. \tag{38}$$

Similarly, based on Eq. (36) and Eq. (37), Eq. (35) and Eq. (37), the coordinates of S can be obtained respectively as

$$x_2 = \frac{b}{1+\tan\theta_2\tan\theta_3}, y_2 = \frac{b\tan\theta_2}{1+\tan\theta_2,\tan\theta_3}, \tag{39}$$

$$x_3 = \frac{b-a\tan\theta_3}{1-\tan\theta_1\tan\theta_3}, y_3 = \frac{a-b\tan\theta_1}{1-\tan\theta_1\tan\theta_3}. \tag{40}$$

Ultimately, based on the results of three cross localization in Eq. (38), Eq. (39) and Eq. (40), the coordinate of $S(x,y)$ can be determined by

$$x = \frac{x_1+x_2+x_3}{3}, y = \frac{y_1+y_2+y_3}{3}. \tag{41}$$

Remark 3: Theoretically, we only need two of the three BSs in Fig. 2 to determine the coordinate of S and achieve the vehicle localization, and the result calculated by Eq. (38), Eq. (39) and Eq. (40) are equal. However, in practice, the coordinates estimated by only two collaborative BSs must exist errors due to various disturbances, and the results of Eq. (38), Eq. (39) and Eq. (40) cannot be completely equal. In this paper, three collaborative BSs are used, in which each two BSs can estimate the coordinates of the target vehicle once. The finally estimated coordinates are averaged by Eq. (41), which can reduce the localization error and make the localization result more stable.

TABLE II
DOA Estimation Results by the Proposed DOA Estimation Approach

Grid interval		DOA 1	DOA 2	DOA 3
$r=1°$	True DOA	$-22.5000°$	$9.9600°$	$36.1900°$
	Estimated DOA	$-22.4988°$	$9.9212°$	$36.2518°$
$r=2°$	True DOA	$-20.8700°$	$1.3900°$	$34.3400°$
	Estimated DOA	$-20.9657°$	$1.4466°$	$34.3429°$
$r=4°$	True DOA	$-22.1800°$	$4.5700°$	$33.3800°$
	Estimated DOA	$-22.1599°$	$4.5272°$	$33.3420°$
$r=6°$	True DOA	$-27.3300°$	$2.1900°$	$36.9100°$
	Estimated DOA	$-27.3579°$	$2.2131°$	$36.9920°$

V. Simulation and Test Results

In this section, the performance of the proposed vehicle localization method is mainly evaluated by the DOA estimation performance of the proposed robust DOA estimation method. The OGSBI [31], ROGSBL [33] and the enhanced SBL method (abbreviated as ESBL) [34] are adopted to compare with the proposed method. In addition, the Cramér-Rao Bound (CRB) is utilized to evaluate the performance of these methods. Each BS in the localization system consists of $M = 8$ transmitting antennas and $N = 10$ receiving antennas, and the distance between adjacent antennas in both transmitting and receiving arrays is half-wavelength. Suppose there exist $K = 3$ un-correlated targets in the same range, and for the sake of generality, their DOAs are randomly generated from $[-30°, -20°]$, $[0°, 10°]$ and $[40°, 50°]$ with a resolution of $0.01°$, respectively. The range from $-90°$ to $90°$

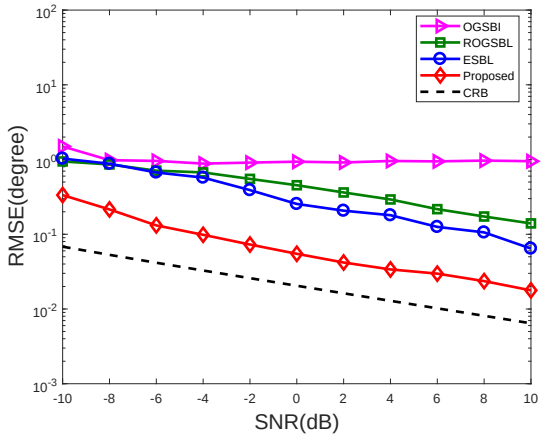

Fig. 4. RMSE versus SNR under non-uniform noise condition

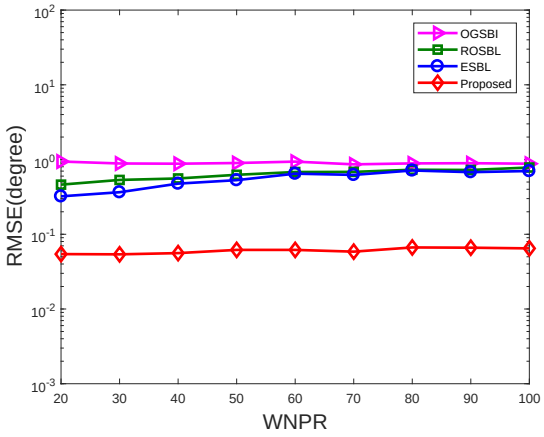

Fig. 6. RMSE versus WNPR under non-uniform noise condition

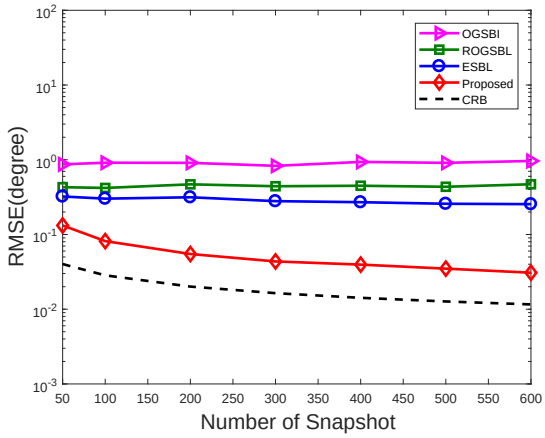

Fig. 5. RMSE versus the number of snapshot under non-uniform noise condition

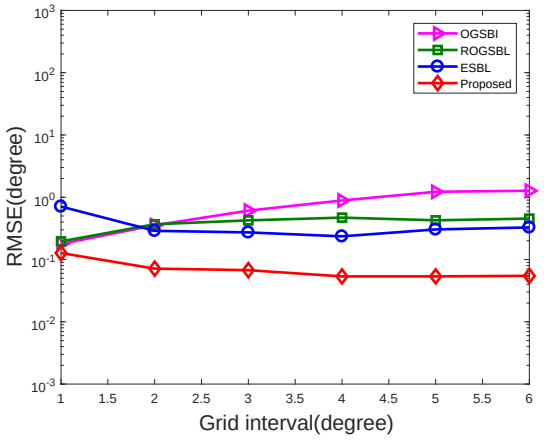

Fig. 7. RMSE versus grid interval under non-uniform noise condition

is uniformly fixed by 4°, which will form a very coarse grid. Except for special instructions, the number of "active" grid points is generally selected as $\eta = P = M + N - 1$, and the covariance matrix of received non-uniform noise is modeled as $\tilde{\boldsymbol{Q}} = diag\{[10, 1, 9, 7, 2, 8, 1.5, 0.5, 1, 3]\}$. The Worst Noise Power Ratio (WNPR) is defined by

$$\text{WNPR} \triangleq \frac{\sigma_{max}^2}{\sigma_{min}^2}, \tag{42}$$

where σ_{max}^2 and σ_{min}^2 represent the maximum value and the minimum value of noise power, respectively. In order to analyze the performance of these methods intuitively, the Root Mean Square Error (RMSE) is defined by

$$\text{RMSE} = \frac{1}{K}\sum_{k=1}^{K}\sqrt{\frac{1}{\xi}\sum_{i=1}^{\xi}\left(\hat{\theta}_{i,k} - \theta_k\right)^2}, \tag{43}$$

where ξ represents the total number of Monte Carlo trials, which is set as $\xi = 100$ in this paper. $\hat{\theta}_{i,k}$ denotes the estimated result of DOA for the kth target in the ith Monte Carlo simulation.

Firstly, the power spectrum of the proposed DOA estimation method with different grid intervals in the case of non-uniform noise (i.e. $\tilde{\boldsymbol{Q}} = diag\{[10, 1, 9, 7, 2, 8, 1.5, 0.5, 1, 3]\}$) is simulated. The results are given in Fig. 3, where the SNR is set as SNR $= 0$dB, and the number of snapshot is $T = 200$. The different grid intervals are set as $r = 1^\circ$, $r = 2^\circ$, $r = 4^\circ$ and $r = 6^\circ$, respectively. As shown in Fig. 3, the power spectrum of the proposed method has very sharp peaks, which can be used to estimate DOA, in the case of different grid intervals. This represents that the proposed method has the advantages of high accuracy and high resolution under the coexistence of non-uniform noise and off-grid error, especially under a very coarse grid condition. On the other hand, the DOA estimation results of Fig. 3 are given in Table II. It can be seen that no matter how large the grid interval is, the proposed method can still maintain high estimation accuracy. This further illustrates that the proposed method can effectively reduce the influence of non-uniform noise and off-grid error, and maintain high DOA estimation accuracy.

Then, the performance of the four methods under different SNRs are compared in the case of non-uniform noise. Fig. 4 shows the change of RMSE versus SNR of four methods, which is carried out under the condition that the number of snapshot is $T = 200$. As shown in Fig. 4, with the increase of SNR, the RMSE of OGSBI almost does not decrease, while

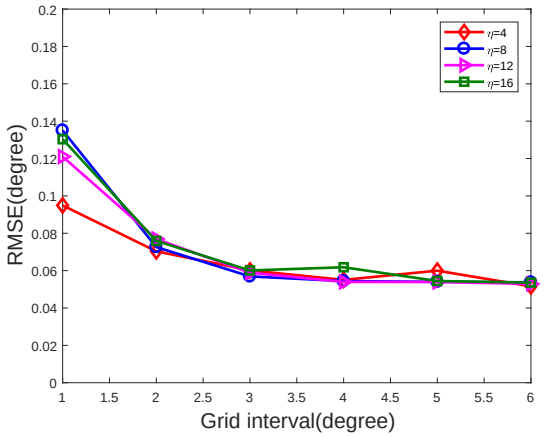

Fig. 8. RMSE versus grid interval with different number of active grid points

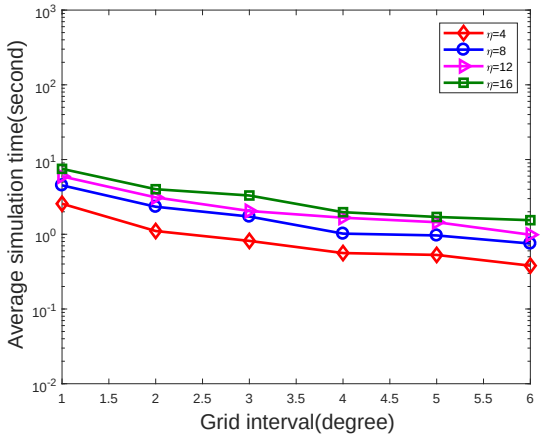

Fig. 9. Average simulation time versus grid interval with different active grid points

that of the other three methods keep decreasing. It is obvious that the proposed method has the lowest RMSE among the four methods, and the RMSE of the proposed method is closer to CRB. The main reason for this result is that the performance of OGSBI in a very coarse grid case is mainly limited by the off-grid error, and the increase of SNR cannot effectively reduce this error. On the other hand, although ROGSBL and ESBL can effectively reduce the off-grid error under coarse grid condition, they ignore the non-uniform noise.

Fig. 5 shows the RMSE versus the number of snapshot in the non-uniform noise case, where SNR $=$ 0dB, $T = 200$. It is clear from Fig. 5 that the performance of the proposed method improves with the increase of the number of snapshots and is more approach CRB. Conversely, the performance of the other three methods do not improve significantly with the increasing number of snapshots. This is due to the existence of non-uniform noise, which is neglected by the other three methods.

Fig. 6 depicts the relationship between RMSE and WNPR with SNR $=$ 0dB and $T = 200$, where WNPR is generated only by changing the maximum value of noise power. It can be observed that the increase of WNPR does not affect RMSE of OGSBI because the off-grid error is dominant in a very coarse grid condition. On the other hand, the RMSE of ROGSBL and ESBL keep increasing with the increase of WNPR, which means that their performance are seriously degraded. While the proposed method always keeps a lowest RMSE at all WNPRs, and its performance is slightly influenced by the non-uniform noise. This is because the proposed method can effectively reduce the influence of non-uniform noise, while the other three methods completely ignore it.

Fig. 7 is the comparison of RMSE of different methods versus different grid intervals in non-uniform noise, where the SNR and snapshot number are respectively set as SNR $=$ 0dB and $T = 200$. As shown in Fig. 7, the proposed method can achieve lower RMSE than the other three methods at all grid interval conditions, especially in a very coarse case, which demonstrates that the proposed method can guarantee the DOA estimation accuracy under the coexistence of off-grid error and non-uniform noise.

Fig. 8 illustrates the RMSE versus grid interval with different number of active grid points, and Fig. 9 illustrates the average simulation time versus grid interval with different number of active grid points, where η is selected as $\eta = 4$, $\eta = 8$, $\eta = 12$ and $\eta = 16$, respectively. Both of these two results are generated in the case of SNR $=$ 0dB and $T = 200$. As shown in Fig. 8, no matter how many activate grid points are selected, the performance of the proposed method can be maintained in almost the same excellent performance. Besides, it can be found from Fig. 9 that the average simulation time decreases with the increase of grid intervals, and the smaller the number of active grid points is, the less the average simulation time needs. The results in Fig. 8 and Fig. 9 demonstrate that the DOA estimation speed of the proposed method can be accelerated by selecting an appropriate number of active grid points and grid interval without affecting the accuracy of DOA estimation.

Finally, the vehicle localization performance of different DOA estimation methods is tested based on the proposed assistant localization system, where $T = 200$, $r = 4^\circ$ and $\eta = P = M + N - 1$. Supposed there exist two vehicles in the same plane range as shown in Fig. 10, their posi-

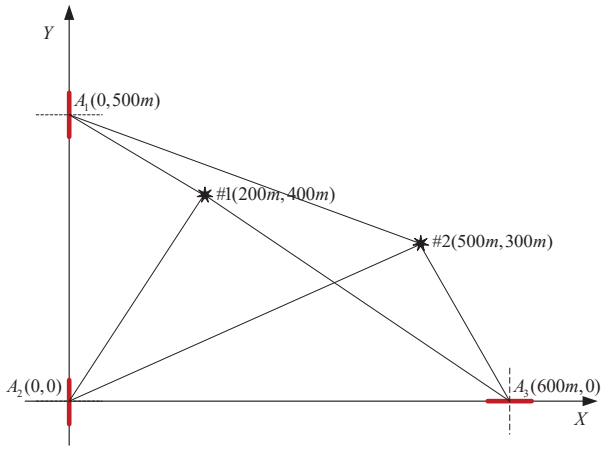

Fig. 10. Localization diagram for two vehicles

TABLE III
VEHICLE LOCALIZATION RESULTS AND ERRORS BY OGSBI

SNR/dB	$(x_{\#1}, y_{\#1})/m$	Error/m	$(x_{\#2}, y_{\#2})/m$	Error/m
-10	(193.30, 399.30)	6.74	(504.67, 294.16)	7.48
-5	(202.61, 394.08)	6.47	(494.92, 305.76)	7.68
0	(194.56, 399.16)	5.51	(505.07, 295.03)	7.10
5	(194.34, 399.32)	5.70	(505.34, 295.00)	7.31
10	(194.24, 399.36)	5.79	(505.48, 294.98)	7.43

TABLE IV
VEHICLE LOCALIZATION RESULTS AND ERRORS BY ROGSBL

SNR/dB	$(x_{\#1}, y_{\#1})/m$	Error/m	$(x_{\#2}, y_{\#2})/m$	Error/m
-10	(193.35, 400.59)	6.68	(503.76, 295.57)	5.81
-5	(195.61 399.17)	4.47	(502.84, 296.66)	4.38
0	(198.51 398.21)	2.34	(502.59, 298.02)	3.26
5	(199.97 398.91)	1.09	(501.12, 299.88)	1.13
10	(199.54 399.73)	0.53	(500.40, 299.51)	0.63

TABLE V
VEHICLE LOCALIZATION RESULTS AND ERRORS BY ESBL

SNR/dB	$(x_{\#1}, y_{\#1})/m$	Error/m	$(x_{\#2}, y_{\#2})/m$	Error/m
-10	(208.13, 394.10)	10.05	(501.65, 305.52)	5.76
-5	(193.05, 405.01)	8.57	(504.45, 297.05)	5.34
0	(195.84, 402.92)	5.08	(500.52, 299.34)	0.84
5	(196.13, 402.87)	4.82	(500.58, 299.44)	0.81
10	(196.90, 401.97)	3.67	(500.29, 299.51)	0.57

TABLE VI
VEHICLE LOCALIZATION RESULTS AND ERRORS BY THE PROPOSED APPROACH

SNR/dB	$(x_{\#1}, y_{\#1})/m$	Error/m	$(x_{\#2}, y_{\#2})/m$	Error/m
-10	(201.88, 400.11)	1.88	(502.40, 299.26)	2.51
-5	(199.70, 398.89)	1.15	(499.27, 300.35)	0.81
0	(200.37, 399.52)	0.60	(500.29, 299.76)	0.37
5	(199.54, 400.12)	0.47	(500.12, 300.22)	0.25
10	(199.76, 400.09)	0.26	(500.04, 299.88)	0.13

tion coordinates are $\#1(200m, 400m)$ and $\#2(500m, 300m)$, respectively. The coordinates of reference points of three BSs are $A_1(0m, 500m)$, $A_2(0m, 0m)$ and $A_3(600m, 0m)$, respectively. Theoretically, the DOAs of these two vehicles with respect to A_1, A_2 and A_3 are $\theta_1^{\#1} = 26.56°$, $\theta_2^{\#1} = 63.43°$, $\theta_3^{\#1} = 45.00°$ and $\theta_1^{\#2} = 21.80°$, $\theta_2^{\#2} = 30.96°$, $\theta_3^{\#2} = 18.43°$. The vehicle localization results and errors versus SNR by different DOA estimation methods are given in Table III, IV, V and VI, respectively. By comparing these results, it can be obviously found that the localization error of our proposed DOA estimation method is the smallest among the four methods, which is consistent with the performance of DOA estimation.

VI. CONCLUSIONS

In this paper, an assistant vehicle localization method based on three collaborative BSs via a robust SBL-based DOA estimation approach is proposed. Through EM algorithm and LS strategy, the power of non-uniform noise and the discrete grid points can be accurately estimated and updated respectively by the proposed robust DOA estimation approach, which enables it to maintain superior DOA estimation performance under the coexistence of non-uniform noise and off-grid error. Based on the collaborative BSs and the proposed DOA estimation approach, the vehicle localization with both off-grid error and non-uniform noise scenario can be accurately achieved. Large number of simulation results have fully demonstrated the effectiveness and superiority of the proposed method. In the future, the proposed vehicle localization method can be combined with the GPS localization to further improve the localization accuracy and real-time localization performance. Thus how to combine the proposed vehicle localization system with GPS system and how to design the localization algorithm is the key problem to be further solved.

ACKNOWLEDGMENT

This work is supported by the National Natural Science Foundation of China (61701144, 61801076), Young Elite Scientists Sponsorship Program by CAST (2018QNRC001), the Program of Hainan Association for Science and Technology Plans to Youth R&D Innovation (QCXM201706), the scientific research projects of University in Hainan Province (Hnky2018ZD-4), the major Science and Technology Project of Hainan Province (ZDKJ2016015), the Scientific Research Setup Fund of Hainan University (KYQD(ZR)1731), the JSPS KAKENHI Grant Number JP16K00117 and the KDDI Foundation.

REFERENCES

[1] K. Ota, M. Dao, V. Mezaris, F.-G.B.-D. Natale, "Deep Learning for Mobile Multimedia: A Survey," *ACM T. Multim. Comput.*, vol. 13, no. 3s, pp. 1-22, Aug. 2017.

[2] L. Li, K. Ota and M. Dong, "HumanLike Driving: Empirical Decision-Making System for Autonomous Vehicles," *IEEE T. Veh. Technol.*, vol. 67, no. 8, pp. 6814-6823, Aug. 2018.

[3] K. Lin and C. Li and G. Fortino and J. J. P. C. Rodrigues, "Vehicle route selection based on game evolution in social internet of vehicles," *IEEE Internet of Things Journal*, vol. 5, no. 4, pp. 2423-2430, Aug. 2018.

[4] L. Guo, M. Dong, K. Ota, Q. Li, T. Ye, J. Wu and J. Li, "A Secure Mechanism for Big Data Collection in Large Scale Internet of Vehicle," *IEEE Internet of Things Journal*, vol. 4, no. 2, pp. 601-610, Apr. 2017.

[5] K. Jo, K. Chu, M. Sunwoo, "GPS-bias correction for precise localization of autonomous vehicles," *2013 IEEE Intell. Vehicles Symp. (IV)*, pp. 636-641, Jun. 2013.

[6] J. K. Suhr, J. Jang, D. Min, H. G. Jung, "Sensor fusion-based low-cost vehicle localization system for complex urban environments," *IEEE Trans. Intell. Transp. Syst.*, vol. 18, no. 5, pp. 1078-1086, May 2017.

[7] H. Li, K. Ota, M. Dong, M. Guo, "Learning Human Activities through Wi-Fi Channel State Information with Multiple Access Points," *IEEE Commun. Mag.*, vol. 56, no. 5, pp. 124-129, May 2018.

[8] I. Bisio, F. Lavagetto M. Marchese, A. Sciarrone, "Energy Efficient WiFi-based Fingerprinting for Indoor Positioning with Smartphones," *2013 IEEE Global Communications Conference (GLOBECOM)*, Dec. 2013.

[9] S. Sadowski, P. Spachos, "RSSI-Based Indoor Localization With the Internet of Things," *IEEE Access*, vol. 6, pp. 30149-30161, Jun. 2018.

[10] J. P. Beaudeau, M.F. Bugallo, P.M. Djuric, "RSSI-based multi-target tracking by cooperative agents using fusion of cross-target information," *IEEE Trans. Signal Process.*, vol. 63, no. 19, pp. 5033-5044, Oct. 2015.
[11] I. Bisio, F. Lavagetto, M. Marchese, A. Sciarrone, "Smart Probabilistic Fingerprinting for WiFi-based Indoor Positioning with Mobile Devices," *Pervasive Mob. Comput.*, vol. 31, pp. 107-123, Sep. 2016.
[12] Y. Zhuang, Y. Li, L. Qi, H. Lan, J. Yang, N. El-Sheimy, "A Two-Filter Integration of MEMS Sensors and WiFi Fingerprinting for Indoor Positioning," *IEEE Sens. J.*, vol. 16, no. 13, pp. 5125-5126, Jul. 2016.
[13] A. Sciarrone, C. Fiandrino, I. Bisio, F. Lavagetto, D. Kliazovich, P. Bouvry, 1.00,0.00,0.00Smart Probabilistic Fingerprinting for Indoor Localization over Fog Computing Platforms," *2016 5th IEEE International Conference on Cloud Networking (Cloudnet)*, Oct. 2016.
[14] H. J.-Rad, G. Leus, "Sparsity-Aware Multi-Source TDOA Localization," *IEEE Trans. on Signal Process.*, vol. 61, no. 19, pp. 4874-4887, Jul. 2013).
[15] B. Huang, L. Xie, Z. Yang, "TDOA-based source localization with distance-dependent noises," *IEEE Trans. Wireless Commun.*, vol. 14, no. 1, pp. 468-480, Jan. 2015.
[16] G. Han, L. Wan, L. Shu, N. Feng, "Two novel DOA estimation approaches for real-time assistant calibration systems in future vehicle industrial," *IEEE Syst. J.*, vol. 11, no. 3, pp. 1361-1372, Sep. 2017.
[17] L. Wan, G. Han, L. Shu, S. Chan, N. Feng, "PD Source Diagnosis and Localization in Industrial High-Voltage Insulation System via Multimodal Joint Sparse Representation," *IEEE Trans. Ind. Electron.*, vol. 63, no. 4, pp. 2506-2516, Jan. 2016.
[18] D. Nion, N. D. Sidiropoulos, "Tensor algebra and multidimensional harmonic retrieval in signal processing for MIMO radar," *IEEE Trans. Signal Process.*, vol. 58, no. 11, pp. 5693-5705, Jul. 2010.
[19] X. Zhang, L. Xu, L. Xu, D. Xu, "Direction of departure (DOD) and direction of arrival (DOA) estimation in MIMO radar with reduced-dimension MUSIC," *IEEE Commun. Lett.*, vol. 14, no. 12, pp. 1161-1163, Nov. 2010.
[20] W. Wang, X. Wang, H. Song, Y. Ma, "Conjugate ESPRIT for DOA estimation in monostatic MIMO radar," *Signal Process.*, vol. 93, no. 7, pp. 2070-2075, Jul. 2013.
[21] J. Li, X. Zhang, W. Chen, "Root-music based angle estimation for MIMO radar with unknown mutual coupling," *Int. J. Antennas Propag.*, vol. 2014, no. 1, pp. 1-8, 2014.
[22] Y. Zhao, P. Shui, H. Liu, "Computationally efficient DOA estimation for MIMO radar," *2009 2nd International Congress on Image and Signal Processing*, pp. 1-3, Oct. 2009.
[23] J. Li, X. Zhang, W. Chen, T. Hu, "Reduced-dimensional ESPRIT for direction finding in monostatic MIMO radar with double parallel uniform linear arrays," *Wirel. Pers. Commun.*, vol. 77, no. 1, pp. 1-19, Jul. 2014.
[24] X. Wang, W. Wang, J. Liu, X. Li, J. Wang, "A sparse representation scheme for angle estimation in monostatic MIMO radar," *Signal Process.*, vol. 104, pp. 258-263, Nov. 2014.
[25] J. Liu, X. Wang, W. Zhou, "Covariance vector sparsity-aware DOA estimation for monostatic MIMO radar with unknown mutual coupling," *Signal Process.*, vol. 119, pp. 21-27, Feb. 2016.
[26] M. E. Tipping, "Sparse Bayesian learning and the relevance vector machine," *J. Mach. Learn. Res.*, vol. 1, no. 3, pp. 211-244, Aug. 2001.
[27] F. Dong, C. Shen, K. Zhang, H. Wang, "Real-Valued Sparse DOA Estimation for MIMO Array System Under Unknown Nonuniform Noise," *IEEE Access*, vol. 6, pp. 52218-52226, Sep. 2018.
[28] Z. Liu, Z. Huang, Y. Zhou, "An efficient maximum likelihood method for direction-of-arrival estimation via sparse Bayesian learning," *IEEE Trans. Wireless Commun.*, vol. 11, no. 10, pp. 1-11, Sep. 2012.
[29] D. Malioutov, M. Çetin, A.S. Willsky, "A sparse signal reconstruction perspective for source localization with sensor arrays," *IEEE Trans. Signal Process.*, vol. 53, no. 8, pp. 3010-3022, Jul. 2005.
[30] H. Zhu, G. Leus, G.B. Giannakis, "Sparsity-cognizant total least-squares for perturbed compressive sampling," *IEEE Trans. Signal Process.*, vol. 59, no. 5, pp. 2002-2016, Feb. 2011.
[31] Z. Yang, L. Xie, C. Zhang, "Off-grid direction of arrival estimation using sparse Bayesian inference," *IEEE Trans. Signal Process.*, vol. 61, no. 1, pp. 38-43, Oct. 2012.
[32] Y. Zhang, Z. Ye, X. Xu, N. Hu, "Off-grid DOA estimation using array covariance matrix and block-sparse Bayesian learning," *Signal Process.*, vol. 98, no. 1, pp. 197-201, May 2014.
[33] J. Dai, X. Bao, W. Xu, C. Chang, "Root sparse Bayesian learning for off-grid DOA estimation," *IEEE Signal Process. Lett.*, vol. 24, no. 1, pp. 46-50, Dec. 2016.
[34] F. Wen, D. Huang, K. Wang, L. Zhang, "DOA estimation for monostatic MIMO radar using enhanced sparse Bayesian learning," *J. Eng.*, vol. 2018, no. 5, pp. 268-273, Jan. 2018.
[35] M. Pesavento, A.B. Gershman, "Maximum-likelihood direction-of-arrival estimation in the presence of unknown nonuniform noise," *IEEE Trans. Signal Process.*, vol. 49, no. 7, pp. 1310-1324, Jul. 2001.
[36] A.B. Gershman, A.L. Matveyev, J.F. Bohme, "Maximum likelihood estimation of signal power in sensor array in the presence of unknown noise field," *IEE Proc. Radar, Sonar and Navigat.*, vol. 142, no. 5, pp. 218-224, Oct. 1995.
[37] D. Madurasinghe, "A new DOA estimator in nonuniform noise," *IEEE Signal Process. Lett.*, vol. 12, no. 4, pp. 337-339, Mar. 2005.
[38] Y. Wu, C. Hou, G. Liao, Q. Guo, "Direction-of-arrival estimation in the presence of unknown nonuniform noise fields," *IEEE J. Ocean. Eng.*, vol. 31, no. 2, pp. 504-510, Oct. 2006.
[39] B. Liao, G.S. Liao, J. Wen, "A method for DOA estimation in the presence of unknown nonuniform noise," *J. Electromagn. Waves. Appl.*, vol. 22, no. 14, pp. 2113-2123, Dec. 2008.
[40] C.E. Chen, F. Lorenzelli, R. E. Hudson, K. Yao, "Stochastic maximum-likelihood DOA estimation in the presence of unknown nonuniform noise," *IEEE Trans. Signal Process.*, vol. 56, no. 7, pp. 3038-3044, Jun. 2008.
[41] P. Yang, Z. Liu, W.L. Jiang, "Improved sparse Bayesian learning method for direction-of-arrival estimation in non-uniform noise," *J. Electromagn. Waves. Appl.*, vol. 28, no. 5, pp. 563-573, Feb. 2014.
[42] P. Stoica, P. Babu, J. Li, "SPICE: Asparse covariance-based estimation method for array processing," *IEEE Trans. Signal Process.*, vol. 59, no. 2, pp. 629-638, Nov. 2010.
[43] Z.Q. He, Z.P. Shi, L. Huang, "Covariance sparsity-aware DOA estimation for nonuniform noise," *Digit. Signal Process.*, vol. 28, no. 1, pp. 75-81, May 2014.
[44] X. Wang, M. Huang, G. Bi, "Sparse Bayesian learning for DOA estimation in MIMO radar with unknown nonuniform noise," *2016 CIE International Conference on Radar (RADAR)*, pp. 1-5, Oct. 2016.

Huafei Wang was born in 1995. He received his B.S.degree at Hainan University, in 2017. Now, he is currently pursuing his M.S. degree in information and communication engineering with Hainan University, Haikou, China. His research interest is array signal processing and MIMO radar.

Liangtian Wan (M'15) received the B.S. degree and the Ph.D. degree in the College of Information and Communication Engineering from Harbin Engineering University, Harbin, China, in 2011 and 2015, respectively. From 2015.10 to 2017.04, he has been a Research Fellow of School of Electrical and Electrical Engineering, Nanyang Technological University, Singapore. He is currently an Associate Professor in School of Software, Dalian University of Technology, China. Dr. Wan has published over 40 scientific papers in international journals and conferences. He is an associate editor of IEEE Access. His research interests include Social Network Analysis and mining, Big Data, Array Signal Processing, Wireless Sensor Networks, Compressive Sensing and its Application.

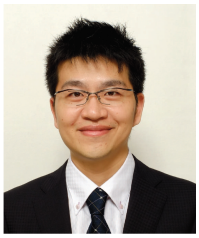

Mianxiong Dong received his B.S., M.S. and Ph.D. degree in Computer Science and Engineering from The University of Aizu, Japan. He is currently an Associate Professor in the Department of Information and Electronic Engineering at the Muroran Institute of Technology, Japan. He was a JSPS Research Fellow with the School of Computer Science and Engineering, The University of Aizu, Japan, and was a visiting scholar with the BBCR group at University of Waterloo, Canada, supported by the JSPS Excellent Young Researcher Overseas Visit Program, from April 2010 to August 2011. Dr. Dong was selected as a Foreigner Research Fellow (a total of 3 recipients all over Japan) by the NEC C&C Foundation in 2011. His research interests include wireless networks, cloud computing, and cyber-physical systems. He has received best paper awards from IEEE HPCC 2008, IEEE ICESS 2008, ICA3PP 2014, GPC 2015, IEEE DASC 2015, IEEE VTC 2016-Fall, FCST 2017, 2017 IET Communications Premium Award and IEEE ComSoc CSIM Best Conference Paper Award 2018. Dr. Dong serves as an Editor for IEEE Transactions on Green Communications and Networking (TGCN), IEEE Communications Surveys and Tutorials, IEEE Network, IEEE Wireless Communications Letters, IEEE Cloud Computing, IEEE Access, as well as a leading guest editor for ACM Transactions on Multimedia Computing, Communications and Applications (TOMM), IEEE Transactions on Emerging Topics in Computing (TETC), IEEE Transactions on Computational Social Systems (TCSS). He has been serving as the Vice Chair of IEEE Communications Society Asia/Pacific Region Information Services Committee and Meetings and Conference Committee, Leading Symposium Chair of IEEE ICC 2019, Student Travel Grants Chair of IEEE GLOBECOM 2019, and Symposium Chair of IEEE GLOBECOM 2016, 2017. He is the recipient of IEEE TCSC Early Career Award 2016, IEEE SCSTC Outstanding Young Researcher Award 2017, The 12th IEEE ComSoc Asia-Pacific Young Researcher Award 2017 and Funai Research Award 2018. He is currently a Member of the Board of Governors and Chair of Student Fellowship Committee of IEEE Vehicular Technology Society.

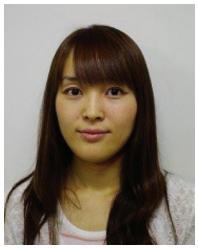

Kaoru Ota was born in Aizu-Wakamatsu, Japan. She received M.S. degree in Computer Science from Oklahoma State University, USA in 2008, B.S. and Ph.D. degrees in Computer Science and Engineering from The University of Aizu, Japan in 2006, 2012, respectively. She is currently an Assistant Professor with Department of Information and Electronic Engineering, Muroran Institute of Technology, Japan. From March 2010 to March 2011, she was a visiting scholar at University of Waterloo, Canada. Also she was a Japan Society of the Promotion of Science (JSPS) research fellow with Kato-Nishiyama Lab at Graduate School of Information Sciences at Tohoku University, Japan from April 2012 to April 2013. Her research interests include Wireless Networks, Cloud Computing, and Cyber-physical Systems. Dr. Ota has received best paper awards from ICA3PP 2014, GPC 2015, IEEE DASC 2015, IEEE VTC 2016-Fall, FCST 2017, 2017 IET Communications Premium Award and IEEE ComSoc CSIM Best Conference Paper Award 2018. She is an editor of IEEE Transactions on Vehicular Technology (TVT), IEEE Communications Letters, Peer-to-Peer Networking and Applications (Springer), Ad Hoc & Sensor Wireless Networks, International Journal of Embedded Systems (Inderscience) and Smart Technologies for Emergency Response & Disaster Management (IGI Global), as well as a guest editor of ACM Transactions on Multimedia Computing, Communications and Applications (leading), IEEE Internet of Things Journal, IEEE Communications Magazine, IEEE Network, IEEE Wireless Communications, IEEE Access, IEICE Transactions on Information and Systems, and Ad Hoc & Sensor Wireless Networks (Old City Publishing). She is the recipient of IEEE TCSC Early Career Award 2017.

Xianpeng Wang was born in 1986. He received his M.S. degree and Ph.D. degree in the College of Automation from Harbin Engineering University (HEU), Harbin, China, in 2012 and 2015, respectively. He was a full-time Research Fellow in the School of Electrical and Electronic Engineering, Nanyang Technological University, Singapore, from 2015 to 2016. Now, he is a professor in the College of Information Science & Technology at Hainan University. He is the author of over 50 papers published in related journals and international conference proceedings, and has served as a reviewer of over 20 journals. His major research interests include communication system, array signal processing, radar signal processing, compressed sensing and its applications.